PHYSICAL REVIEW VOLUME 173, NUMBER 3 15 SEPTEMBER 1968

Optical Phonons and Dynamic Charge in Trigonal Se and Te

INAN CHEN AND RICHARD ZALLEN
Research Laboratories, Xerox Corporation, Rochester, New York 14603

(Received 10 April 1968)

Lattice vibrations in elemental crystals can possess a first-order electric moment, and thus exhibit one-phonon infrared absorption (reststrahlen), by the mechanism of displacement-induced charge redistribution (dynamic charge). Trigonal Se and Te, with three atoms per unit cell, belong to the simplest class of reststrahlen-displaying elemental crystals. We have performed a group-theoretical, shell-model analysis of the zone-center optical phonons in these monatomic semiconductors using the most general dynamical matrix consistent with crystal symmetry and translational invariance. The dynamic charges associated with the infrared-active modes have been derived, and the effective-charge tensor $(\partial \mathbf{p}/\partial \mathbf{u})$ constructed. In this model the macroscopic polarization is associated entirely with the shell motion, and the three independent entries appearing in the effective-charge tensor correspond to coupling coefficients connecting acoustical shell displacements with optical core displacements. For the A_2 mode, the chain-twisting core motion induces an axial shell motion responsible for the electric moment so that a vibration with atomic displacements $\perp c$ interacts with radiation polarized $\| c$. For this mode both dynamic charge and restoring force depend upon next-nearest-neighbor interactions between chains, and vanish in the limit of isolated chains. The expressions obtained for the two E-mode effective charges provide a means for understanding the small oscillator strength observed for one E-mode pair in both Se and Te. The lattice sums entering into the long-range electrostatic interaction matrix have been evaluated numerically for the detailed geometry of both crystals. In addition, a simple central-force model for the short-range interactions is discussed to illustrate some of the more generally derived results.

1. INTRODUCTION

LATTICE vibrations in elemental, non-metallic crystals have been most heavily investigated for the cubic group-IV semiconductors C, Si, and Ge. Recently, infrared (ir) and Raman measurements of zone-center optical phonons have been reported for the trigonal group-VI semiconductors Se and Te.[1-4] Long-wavelength optical vibrations in these crystals, which are the subject of this paper, differ in a fundamental respect from optical vibrations in the familiar germanium-family diamond-structure crystals: *For* Se *and* Te, *some optical modes are ir-active.* Se and Te exhibit pronounced one-phonon absorption spectra (reststrahlen), while C, Si, and Ge do not. The reason for the nonoccurrence of reststrahlen in diamond-structure crystals, first stated by Lax and Burstein[5] in 1955, is discussed in the preceding article[6] in which the following generalization is derived: A necessary and sufficient condition for the existence of reststrahlen in an elemental crystal is a structure with at least three atoms in the primitive unit cell, $s \geq 3$. For diamond-structure crystals $s=2$, so that the optical modes are infrared-inactive. The crystal structure of trigonal Se and Te, with $s=3$, is the simplest structure known to occur which satisfies this minimum-complexity condition for a reststrahlen-displaying elemental crystal. The purpose of this paper is to present a treatment of the lattice dynamics of Se and Te in the simplest manner which includes the occurrence of allowed one-phonon absorption processes, a very strong effect in these crystals.

For NaCl-type ionic crystals, the first-order electric moment (moment linear in the atomic displacements) responsible for reststrahlen can be very well understood in terms of relative motions of nearly-rigid positive and negative ions,[7] with a small correction coming from the finite deformability of the charge distribution about each ion. For an elemental crystal possessing a first-order moment, the oscillating dipole is due entirely to the latter phenomenon: the deformation or rearrangement of the electronic charge distribution, under the influence of bonding interactions, induced by the atomic displacements during vibration. The effective charge (e^*) associated with displacement-induced charge redistribution is sometimes referred to as dynamic charge,[8] to distinguish it from the static (or ionic) charge associated with the undisplaced atoms in NaCl-type crystals.

Previous treatments of lattice vibrations in Se and Te,[4,9] aimed at calculating phonon frequencies and dispersion curves from a (hopefully) small number of force-constant parameters, have considered effective atom-atom interactions between neutral, rigid atoms. Since we are interested in dipole moments and effective

---

[1] P. Grosse, M. Lutz, and W. Richter, Solid State Commun. 5, 99 (1967).

[2] G. Lucovsky, R. C. Keezer, and E. Burstein, Solid State Commun. 5, 439 (1967).

[3] A. Mooradian and G. B. Wright, in Proceedings of the International Conference on the Physics of Selenium and Tellurium, Montreal, 1967 (unpublished).

[4] R. Geick, U. Schröder, and J. Stuke, Phys. Status Solidi 24, 99 (1967); R. Geick and U. Schröder (unpublished).

[5] M. Lax and E. Burstein, Phys. Rev. 97, 39 (1955); M. Lax, Phys. Rev. Letters 1, 131 (1958); 1, 133 (1958).

[6] R. Zallen, preceding paper, Phys. Rev. 173, 824 (1968).

[7] M. Born and K. Huang, *Dynamical Theory of Crystal Lattices* (Oxford University Press, London, 1954).

[8] E. Burstein, M. H. Brodsky, and G. Lucovsky, Intern. J. Quantum Chem. 1S, 759 (1967); W. Cochran, Nature 191, 60 (1961).

[9] M. Hulin, Ann. Phys. (Paris) 8, 647 (1963); M. Hulin, in *Proceedings of the International Conference on Lattice Dynamics, Copenhagen, 1963*, edited by R. F. Wallis (Pergamon Press, Ltd., London, 1965), p. 135.

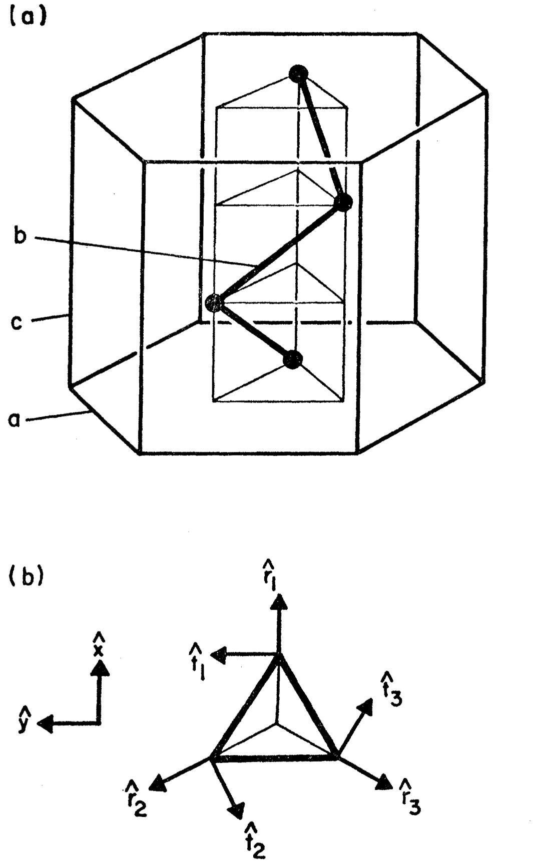

FIG. 1. (a) Primitive unit cell for the crystal structure of trigonal Se and Te; (b) coordinate axes, viewed along the c axis ($=z$ axis), used to describe the atomic displacements.

charges, we must go to the next higher approximation, the shell model, in which the atoms are resolved into rigid, oppositely-charged cores and shells.[10,11] The shell model was originally introduced by Dick and Overhauser[10] in order to elucidate, in a simple manner, the role of dynamic charge in the alkali halides in producing the well-known deviation of e^*/e from 1, the rigid-ion value for those crystals. Here we apply the shell model to Se and Te in order to elucidate the manner in which charge deformation produces the observed deviation of e^*/e from *zero*, the rigid-ion value for elemental crystals.

The group-theoretical reduction of the dynamical matrix is performed in Sec. 2 and the analysis is carried over to the shell model in Sec. 3. Sections 4 and 5 present detailed treatments of the infrared-active optical modes, particularly the nondegenerate A_2 mode in which the vibration-induced polarization is perpendicular to the atomic displacements. The dynamic charges are derived in terms of shell-model matrix elements and collected in the effective charge tensor $(\partial\mathbf{p}/\partial\mathbf{u})$ shown in Sec. 6. In this section we also discuss optical polarizability and Raman scattering. The geometry-determined part of the long-range electrostatic interaction is calculated in Sec. 7 for both Se and Te, and in Sec. 8 we illustrate some of the earlier results by means of a simple model for the short-range forces. The principal results are summarized in Sec. 9.

2. DYNAMICAL MATRIX FOR Se AND Te

In this section we use group-theoretical methods to obtain the structure of the most general dynamical matrix consistent with the crystal symmetry of trigonal Se and Te. The introduction of the dynamical matrix, which specifies the interactions between atoms in the harmonic approximation, follows Born and Huang,[7] whose notation we adhere to when possible. The application of group theory to a nonsymmorphic structure requires care in describing interchanges among sublattices, but is otherwise straightforward. The method has recently been described in clear detail by Chen in an analysis of lattice vibrations in white tin,[12] a nonsymmorphic structure with $s=2$.

Let $\mathbf{x}(l,k)$ and $\mathbf{u}(l,k)$ denote the equilibrium position and the displacement from equilibrium, respectively, of atom k in unit cell l in a crystal containing N primitive unit cells with s atoms per cell. The translational normal coordinate (TNC,[12] analog of a Bloch function) of wave vector $\mathbf{q}$ is defined as

$$\mathbf{u}(\mathbf{q},k)=\frac{1}{\sqrt{N}}\sum_l \mathbf{u}(l,k)\exp[-i\mathbf{q}\cdot\mathbf{x}(l,k)], \qquad (2.1)$$

and the inverse relation is

$$\mathbf{u}(l,k)=\frac{1}{\sqrt{N}}\sum_q \mathbf{u}(\mathbf{q},k)\exp[i\mathbf{q}\cdot\mathbf{x}(l,k)]. \qquad (2.2)$$

We avoid absorbing the customary mass factor $(\sqrt{m_k})$ into the definition of the TNC's in order to facilitate the transition to the shell model in subsequent sections.

The s 3-dimensional vectors $\mathbf{u}(\mathbf{q},k)$ define a $3s$-dimensional vector $\mathbf{u}(\mathbf{q})$, in terms of which the equation of motion for plane waves of wave-vector $\mathbf{q}$ and angular frequency ω becomes

$$\mathbf{M}\omega^2\mathbf{u}(\mathbf{q})=\mathbf{D}(\mathbf{q})\mathbf{u}(\mathbf{q}), \qquad (2.3)$$

where $\mathbf{M}$ and $\mathbf{D}$ are $3s\times 3s$ matrices. (Throughout this paper we will use boldface lower-case letters for vectors, boldface capitals for matrices.) $\mathbf{M}$ is a diagonal matrix with elements given by $m_k\delta_{kk'}\delta_{\alpha\alpha'}$, where $k\alpha$ labels the α component of the displacement of atom k. $\mathbf{D}$ is the

---

[10] B. G. Dick and A. W. Overhauser, Phys. Rev. **112**, 90 (1958).

[11] R. A. Cowley, Proc. Roy. Soc. (London) **A268**, 109 (1962); **A268**, 121 (1962); R. A. Cowley, W. Cochran, B. N. Brockhouse, and A. D. B. Woods, Phys. Rev. **131**, 1030 (1963); R. L. Marston and B. G. Dick, Solid State Commun. **5**, 731 (1967).

[12] S. H. Chen, Phys. Rev. **163**, 532 (1967).

Table I. Symmetrized coordinates.

I.R.	Basis vectors	Dynamical matrix								
A_1	$\mathbf{e}_1=(\frac{1}{3})^{1/2}[\hat{r}_1+\hat{r}_2+\hat{r}_3]$	D_{11}								
A_2	$\mathbf{e}_2=(\frac{1}{3})^{1/2}[\hat{t}_1+\hat{t}_2+\hat{t}_3]$		D_{22}	D_{23}						
A_2	$\mathbf{e}_3=(\frac{1}{3})^{1/2}[\hat{z}_1+\hat{z}_2+\hat{z}_3]$		D_{23}	D_{33}						
E	$\mathbf{e}_4=(\frac{1}{12})^{1/2}[2\hat{r}_1-\hat{r}_2-\sqrt{3}\hat{t}_2-\hat{r}_3+\sqrt{3}\hat{t}_3]$				D_{44}	D_{45}	D_{46}			
E	$\mathbf{e}_5=(\frac{1}{12})^{1/2}[2\hat{r}_1-\hat{r}_2+\sqrt{3}\hat{t}_2-\hat{r}_3-\sqrt{3}\hat{t}_3]$				D_{45}	D_{55}	D_{56}			
E	$\mathbf{e}_6=(\frac{1}{2})^{1/2}[\hat{z}_2-\hat{z}_3]$				D_{46}	D_{56}	D_{66}			
E	$\mathbf{e}_7=(\frac{1}{12})^{1/2}[2\hat{t}_1+\sqrt{3}\hat{r}_2-\hat{t}_2-\sqrt{3}\hat{r}_3-\hat{t}_3]$							D_{44}	D_{45}	D_{46}
E	$\mathbf{e}_8=(\frac{1}{12})^{1/2}[-2\hat{t}_1+\sqrt{3}\hat{r}_2+\hat{t}_2-\sqrt{3}\hat{r}_3+\hat{t}_3]$							D_{45}	D_{55}	D_{56}
E	$\mathbf{e}_9=(\frac{1}{6})^{1/2}[-2\hat{z}_1+\hat{z}_2+\hat{z}_3]$							D_{46}	D_{56}	D_{66}

dynamical matrix, a lattice sum of force constants:

$$\mathbf{D}_{k\alpha,k'\alpha'}(\mathbf{q})=\sum_l \mathbf{\Phi}_{k\alpha,k'\alpha'}(l)\times\exp[-i\mathbf{q}\cdot\{\mathbf{x}(l,k)-\mathbf{x}(0,k')\}],$$

$$\mathbf{\Phi}_{k\alpha,k'\alpha'}(l)=\left(\frac{\partial^2\mathbf{\Phi}}{\partial u_\alpha(l,k)\partial u_{\alpha'}(0,k')}\right)_0, \tag{2.4}$$

where $\mathbf{\Phi}$ is the potential function of the atomic coordinates. We are primarily concerned here with long-wavelength vibrations ($\mathbf{q}\approx 0$) for which $\mathbf{D}$ is real and the full crystal symmetry is maintained.

The three-atom unit cell of Se and Te is shown in Fig. 1.[13] The structure consists of helical coils ("chains") which wind around the screw triad axis, the *c* axis of the crystal. The helices contain three atoms per turn and are in hexagonal array. The space group is $P3_121$ (D_3^4) for the right-handed crystal of Fig. 1[14] and the six operations of the factor group are[15] 1, 3_1, $3_1\times 3_1$, 2, $3_1\times 2$, and $2\times 3_1$, where

1 denotes the identity;

3_1 denotes a threefold rotation about the *c* axis, followed by a $\frac{1}{3}c$ translation parallel to the axis;

2 denotes a twofold rotation about an axis perpendicular to *c*.

This group has been discussed by several authors.[9,16,17] It is simply isomorphic to the familiar group $3m$ (C_{3v}) of the equilateral triangle and possesses three irreducible representations (I.R.'s): two 1-dimensional I.R.'s, symmetric (A_1) and antisymmetric (A_2); and a 2-dimensional I.R. (E).[18] Notations other than A_1,A_2,E which have also been used for the Γ-point ($\mathbf{q}=0$) I.R.'s are $\Gamma_1,\Gamma_{1'},\Gamma_2$ [9] and $\Gamma_1,\Gamma_2,\Gamma_3$.[16]

The radial ($\hat{r}_i$), tangential ($\hat{t}_i$), and axial ($\hat{z}_i$) unit vectors shown in Fig. 1 are convenient bases for discussing the 9-dimensional representation Γ generated by the unit-cell atomic coordinates. The matrices representing 3_1 and 2, the group generators, in this system are

$$\mathbf{S}^\Gamma(3_1)=\begin{bmatrix}0 & \mathbf{S}^P(3_1) & 0\\ 0 & 0 & \mathbf{S}^P(3_1)\\ \mathbf{S}^P(3_1) & 0 & 0\end{bmatrix}$$

and

$$\mathbf{S}^\Gamma(2)=\begin{bmatrix}\mathbf{S}^P(2) & 0 & 0\\ 0 & 0 & \mathbf{S}^P(2)\\ 0 & \mathbf{S}^P(2) & 0\end{bmatrix}, \tag{2.5}$$

where the 3×3 submatrices are

$$\mathbf{S}^P(3_1)=\begin{bmatrix}1 & 0 & 0\\ 0 & 1 & 0\\ 0 & 0 & 1\end{bmatrix} \text{ and } \mathbf{S}^P(2)=\begin{bmatrix}1 & 0 & 0\\ 0 & -1 & 0\\ 0 & 0 & -1\end{bmatrix}. \tag{2.6}$$

The reduction of this representation yields

$$\Gamma=A_1+2A_2+3E, \tag{2.7}$$

which specifies the symmetries of the 9 zone-center phonons.

Combining the above $\mathbf{S}^\Gamma$ matrices with the I.R. matrices[18] in the method of projection operators,[19] symmetrized combinations of atomic coordinates can be constructed; the results, in terms of $\hat{r}_i,\hat{t}_i,\hat{z}_i$, are given in Table I. Henceforth we will use these symmetrized basis vectors in discussing the secular equation (2.3).

In symmetrized coordinates, the dynamical matrix is block-diagonalized. The symmetry-determined form of $\mathbf{D}$ is shown in Table I. $\mathbf{D}$ is symmetric, so that the number of independent elements in the initial 9×9 matrix, before invoking crystal symmetry, is 45 rather than 81. The number of independent elements in the block-diagonalized matrix of Table I is 10. This reduction is obtained by the requirement that $\mathbf{D}$ commute with each $\mathbf{S}^\Gamma$. [It is sufficient to use $\mathbf{S}^\Gamma(3_1)$ and $\mathbf{S}^\Gamma(2)$, since 3_1 and 2 are group generators.]

An additional set of constraints, not yet taken into account in Table I, is provided by translational invariance, the requirement of a vanishing restoring force for a uniform translation of the lattice. Unit rigid

---

[13] R. W. G. Wyckoff, *Crystal Structures* (Interscience Publishers, New York, 1963), Vol. I, p. 36.

[14] For the enantiomorphic left-handed form, the space group is $P3_221$ (D_3^6).

[15] *International Tables for X-Ray Crystallography, Symmetry Groups* (Kynoch Press, Birmingham, England, 1952), Vol. I, p. 257.

[16] R. H. Asendorf, J. Chem. Phys. **27**, 11 (1957).

[17] A. Nussbaum, in *Solid State Physics*, edited by F. Seitz and D. Turnbull (Academic Press Inc., New York, 1966), Vol. 18, p. 225.

[18] V. Heine, *Group Theory in Quantum Mechanics* (Pergamon Press, Ltd., London, 1960), p. 27.

[19] G. F. Koster, MIT Solid State and Molecular Theory Group, Technical Report No. 8, 1956 (unpublished).

translations of $\hat{x}$, $\hat{y}$, and $\hat{z}$ (cartesian coordinates also shown in Fig. 1) correspond to $\mathbf{u}=\sqrt{3}\mathbf{e}_4$, $\sqrt{3}\mathbf{e}_7$, and $\sqrt{3}\mathbf{e}_3$, respectively, in symmetrized coordinates. Translational invariance then requires that

$$\mathbf{D}\mathbf{e}_3=\mathbf{D}\mathbf{e}_4=\mathbf{D}\mathbf{e}_7=0\,, \tag{2.8}$$

leading to

$$D_{ij}=0 \quad \text{for} \quad ij=23,33,44,45,46. \tag{2.9}$$

The three zeros on the diagonal ($D_{33},D_{44},D_{77}=D_{44}$) correspond, of course, to the zone-center acoustical phonons.

The block-diagonalized structure of $\mathbf{D}$ exhibits a 1×1 A_1 block, a 2×2 A_2 block, and two identical 3×3 E blocks. The two E blocks show that eigenvectors of E symmetry occur in degenerate pairs, so that if a given combination of $\mathbf{e}_4$, $\mathbf{e}_5$, and $\mathbf{e}_6$ comprises an eigenvector of eigenfrequency ω, the same combination of $\mathbf{e}_7$, $\mathbf{e}_8$, and $\mathbf{e}_9$ defines an eigenfrequency at the same ω. The form of $\mathbf{D}$ in Table I demonstrates immediately that $\mathbf{e}_1$ (a "chain-breathing" motion of frequency $[D_{11}/m]^{1/2}$) is an eigenvector determined by symmetry, while $\mathbf{e}_2$ and $\mathbf{e}_3$, and similarly $\mathbf{e}_4$, $\mathbf{e}_5$, and $\mathbf{e}_6$, may be mixed among themselves by the 2×2 and 3×3 blocks, respectively. However, translational invariance (2.8–9) reveals that the 2×2 A_2 block contains only one nonvanishing element so that $\mathbf{e}_2$ and $\mathbf{e}_3$ are, in fact, symmetry-determined eigenvectors; $\mathbf{e}_3$ is the acoustical mode polarized $\|c$, while $\mathbf{e}_2$ (a "chain-twisting" motion) is an optical mode of frequency $[D_{22}/m]^{1/2}$. Similarly $\mathbf{e}_4$ and $\mathbf{e}_7$, which form one of the three pairs of E modes, are acoustical phonons polarized $\perp c$. The other two pairs of E modes, two combinations of $\mathbf{e}_5$ and $\mathbf{e}_6$ degenerate with the same combinations of $\mathbf{e}_8$ and $\mathbf{e}_9$, are not determined by symmetry alone. These optical vibrations, unlike the A_1 and A_2 optical modes ($\mathbf{e}_1$ and $\mathbf{e}_2$), involve atomic motions with components both parallel and perpendicular to the c axis.

3. SHELL-MODEL DYNAMICAL MATRIX

In the shell model for an elemental crystal, each atomic site is associated with two particles: a core (nucleus plus tightly-bound electrons) of mass m, charge $+Ze$, and a very light shell of mass m^*, charge $-Ze$. For trigonal Se and Te, the unit cell of Fig. 1 then contains 6 particles and the secular equation (2.3) couples 18 coordinates: $\mathbf{e}_1,\mathbf{e}_2,\cdots\mathbf{e}_9$ for the cores; $\mathbf{e}_1^*,\mathbf{e}_2^*,\cdots\mathbf{e}_9^*$ for the shells. In these symmetrized coordinates, the 18×18 shell-model dynamical matrix takes on the appearance

$$\mathbf{D}=\begin{pmatrix}\mathbf{D}^{cc} & \mathbf{D}^{cs}\\ \mathbf{D}^{sc} & \mathbf{D}^{ss}\end{pmatrix}, \tag{3.1}$$

where each of the three symmetric 9×9 submatrices, $\mathbf{D}^{cc}$, $\mathbf{D}^{cs}=\mathbf{D}^{sc}$, and $\mathbf{D}^{ss}$, are of the form shown in Table I. The $\mathbf{D}$ of (3.1) may be put into block-diagonalized form by simply collecting symmetries and rearranging rows and columns to correspond to the order $\mathbf{e}_1,\mathbf{e}_1^*,\mathbf{e}_2,\mathbf{e}_2^*,\cdots\mathbf{e}_9,\mathbf{e}_9^*$ instead of $\mathbf{e}_1,\mathbf{e}_2,\cdots\mathbf{e}_9,\mathbf{e}_1^*,\mathbf{e}_2^*,\cdots\mathbf{e}_9^*$.

The number of independent elements of $\mathbf{D}$, thus far reduced to 30 (10 for each submatrix) by crystal symmetry, can be further reduced, as in the last section, by translational invariance. Relations (2.8) and (2.9) become, in the shell model,

$$\mathbf{D}(\mathbf{e}_3+\mathbf{e}_3^*)=\mathbf{D}(\mathbf{e}_4+\mathbf{e}_4^*)=\mathbf{D}(\mathbf{e}_7+\mathbf{e}_7^*)=0 \tag{3.2}$$

and

$$D_{ij}^{cc}=D_{ij}^{ss}=-D_{ij}^{cs} \quad \text{for} \quad ij=23,33,44,45,46. \tag{3.3}$$

The 10 relations of (3.3) reduce the number of independent elements to 20: 3 in the 2×2 A_1 block, 5 in the 4×4 A_2 block, and 12 in either 6×6 E block.

The A_2 and E optical phonons are treated in the next two sections, with special attention to the dynamic charge associated with these ir-active modes. The procedure is illustrated below for the simple case of the A_1 mode.

For A_1 symmetry the shell-model equation of motion is

$$\begin{pmatrix}m & 0\\ 0 & m^*\end{pmatrix}\omega^2\begin{pmatrix}s_1\\ s_1^*\end{pmatrix}=\begin{pmatrix}D_{11}^{cc} & D_{11}^{cs}\\ D_{11}^{cs} & D_{11}^{ss}\end{pmatrix}\begin{pmatrix}s_1\\ s_1^*\end{pmatrix}, \tag{3.4}$$

where s_1 and s_1^* are the core and shell coordinates, $\mathbf{u}=s_1\mathbf{e}_1+s_1^*\mathbf{e}_1^*$. At phonon frequencies $m^*\omega^2$ is negligible ($m^*/m\sim10^{-5}$), so that we may set $m^*\omega^2=0$.[20] The vibrational eigenvector and eigenfrequency are then given by

$$s_1^*=a_{11}s_1\,,\quad a_{11}=-D_{11}^{cs}/D_{11}^{ss}; \tag{3.5}$$

and

$$m\omega^2=\lambda_{11}\,,\quad \lambda_{11}=(D_{11}^{cc}D_{11}^{ss}-D_{11}^{cs2})/D_{11}^{ss}. \tag{3.6}$$

The coupling coefficient a_{11} specifies the amount of shell motion induced by the atomic vibration (core motion).

The electric moment associated with each vibration is determined by

$$\mathbf{p}(\mathbf{q})=\sum_k\left[+Ze\mathbf{u}(\mathbf{q},k)-Ze\mathbf{u}^*(\mathbf{q},k)\right], \tag{3.7}$$

where the first term represents the contribution of the cores and the second term that of the shells, with the sum taken over the three atomic sites in the unit cell. In the present case, from the definition of $\mathbf{e}_1$ (and similarly $\mathbf{e}_1^*$) given in Table I, we see that $\mathbf{p}$ vanishes for the zone-center A_1 mode; this fully-symmetric vibration is ir-inactive (a statement deducible directly from group theory).[21]

---

[20] The effect of setting $m^*\omega^2=0$ is to discard the high-frequency solution of (3.4) which corresponds to a shell vibration (i.e., an electronic excitation) rather than a lattice vibration. The extra eigenfrequencies, which are introduced in the doubling of $\mathbf{D}$ upon going to the shell model, are subsequently eliminated in this way.

[21] Reference 6, Table I.

4. A_2-SYMMETRY OPTICAL MODE

The shell-model equation of motion in the A_2 subspace spanned by $s_2\mathbf{e}_2+s_3\mathbf{e}_3+s_2^*\mathbf{e}_2^*+s_3^*\mathbf{e}_3^*$ is

$$\omega^2\begin{bmatrix} m & & & \\ & m & & \\ & & m^* & \\ & & & m^* \end{bmatrix}\begin{bmatrix} s_2 \\ s_3 \\ s_2^* \\ s_3^* \end{bmatrix}$$

$$=\begin{bmatrix} D_{22}{}^{cc} & D_{23}{}^{cc} & D_{22}{}^{cs} & -D_{23}{}^{cc} \\ D_{23}{}^{cc} & D_{33}{}^{cc} & -D_{23}{}^{cc} & -D_{33}{}^{cc} \\ D_{22}{}^{cs} & -D_{23}{}^{cc} & D_{22}{}^{ss} & D_{23}{}^{cc} \\ -D_{23}{}^{cc} & -D_{33}{}^{cc} & D_{23}{}^{cc} & D_{33}{}^{cc} \end{bmatrix}\begin{bmatrix} s_2 \\ s_3 \\ s_2^* \\ s_3^* \end{bmatrix}. \quad (4.1)$$

Setting $m^*=0$ in the third and fourth rows leads to relations for the shell displacements in terms of core displacements:

$$s_2^*=a_{22}s_2\,, \qquad a_{22}=\frac{D_{23}{}^{cc^2}+D_{22}{}^{cs}D_{33}{}^{cc}}{D_{23}{}^{cc^2}-D_{22}{}^{ss}D_{33}{}^{cc}}; \quad (4.2)$$

$$s_3^*=a_{32}s_2+s_3\,, \quad a_{32}=\frac{D_{23}{}^{cc}(D_{22}{}^{cs}+D_{22}{}^{ss})}{D_{22}{}^{ss}D_{33}{}^{cc}-D_{23}{}^{cc^2}}$$

$$=(1-a_{22})\frac{D_{23}{}^{cc}}{D_{33}{}^{cc}}. \quad (4.3)$$

The second and first rows, respectively, of (4.1) then yield

$$m\omega^2 s_3=0 \quad (4.4)$$

and

$$m\omega^2 s_2=\lambda_{22}s_2\,, \quad (4.5)$$

where

$$\lambda_{22}=\frac{1}{D_{23}{}^{cc^2}-D_{22}{}^{ss}D_{33}{}^{cc}}\big[D_{23}{}^{cc^2}(D_{22}{}^{cc}+2D_{22}{}^{cs}+D_{22}{}^{ss})$$

$$+D_{33}{}^{cc}(D_{22}{}^{cs^2}-D_{22}{}^{cc}D_{22}{}^{ss})\big]. \quad (4.6)$$

One solution of (4.2–6) is immediately recognizable as an acoustical mode:

$$\omega=0, \quad s_2=s_2^*=0, \quad s_3=s_3^*. \quad (4.7)$$

This corresponds to a rigid translation of the crystal parallel to the c axis.

For the optical mode, by (4.4), s_3 vanishes, while the other three coordinates participate in the vibration:

$$\omega=(\lambda_{22}/m)^{1/2}, \quad (4.8)$$

$$s_3=0, \quad s_2^*=a_{22}s_2, \quad s_3^*=a_{32}s_2. \quad (4.9)$$

The last relation shows that in this mode the atomic motion, a chain rotation ($s_2\mathbf{e}_2$), induces not only a similar motion of the shells ($s_2^*\mathbf{e}_2^*$) but in addition, via the coupling coefficient a_{32}, an axial motion of the shells ($s_3^*\mathbf{e}_3^*$). We will see below that it is precisely this *axial shell motion* which accounts for the electric moment of the A_2 optical mode, a dipole moment at first sight mysterious since, being parallel to the c axis, it is perpendicular to the displacements of all of the atoms (cores) in this mode.

From (3.7) and Table I, the unit-cell moment of an A_2 vibration is $\mathbf{p}=p_z\hat{z}$, with

$$p_z=\sqrt{3}Ze(s_3-s_3^*); \quad (4.10)$$

axial displacements (s_3,s_3^*) contribute to $\mathbf{p}$, while chain-twist displacements (s_2,s_2^*) do not. We check, with (4.7), that $\mathbf{p}$ vanishes for the acoustical mode, as it must by charge neutrality. For the optical mode we find that

$$\begin{aligned} p_z&=-\sqrt{3}Zes_3^* \\ &=-\sqrt{3}Zea_{32}s_2\,, \end{aligned} \quad (4.11)$$

verifying the central role of the induced axial motion of the shells. We identify the multiplier of s_2 in (4.11) with the effective charge of the optical mode of A_2 symmetry:

$$e^*(A_2)=-\sqrt{3}Zea_{32}. \quad (4.12)$$

The interpretation of these results is illustrated in Fig. 2. An interesting feature of the "chain-twisting" A_2 mode is that for this vibration both the restoring force and the induced electric moment depend upon the presence of next-nearest-neighbor (NNN), and higher-order, interatomic interactions. (This point is discussed further in Sec. 8 in terms of a simple model for the short-range interactions.) Nearest-neighbor (NN) bond lengths and angles are unchanged during this vibration. Equilibrium NN bonds are shown as solid lines in Fig. 2. Shown as dashed lines are the instantaneous locations of the four NNN bonds surrounding one atom. For the s_2 displacement shown, bonds 1 and 2 are in compression, bonds 3 and 4 in tension, relative to their equilibrium lengths. These interchain bonds, viewed as springs, provide a restoring force opposing s_2, contributing importantly to λ_{22}.

The shell-model results of (4.9) are represented on the left side of Fig. 2, with heavy dots as cores, open circles as shells, and arrows as the dipoles induced at the atomic sites by the A_2 optical eigenvibration. The significance of the coupling coefficients a_{22} and a_{32}, which specify shell displacements induced by core displacements, is evident. The dipole components in the plane $\perp c$ sum to zero over the unit cell, while the components $\| c$ are equal and add to give the result of (4.11).

As nearest-neighbor interactions do not contribute to λ_{22}, we might expect $\omega(A_2)$ to be smaller than the other optical-mode eigenfrequencies. This is indeed the case, for both Se and Te.[1–4] However the analogous statement for the first-order moment does not hold. The $e^*(A_2)$ derived from the reststrahlen band for light polarized parallel to the c axis ($\mathbf{E}\| c$) is as large ($\sim e$) as the effective charges for the E-mode reststrahlen bands observed for $\mathbf{E}\perp c$.[2,4] We conclude that next-nearest-neighbor interactions contribute substantially to the dynamic charge of their-active modes.

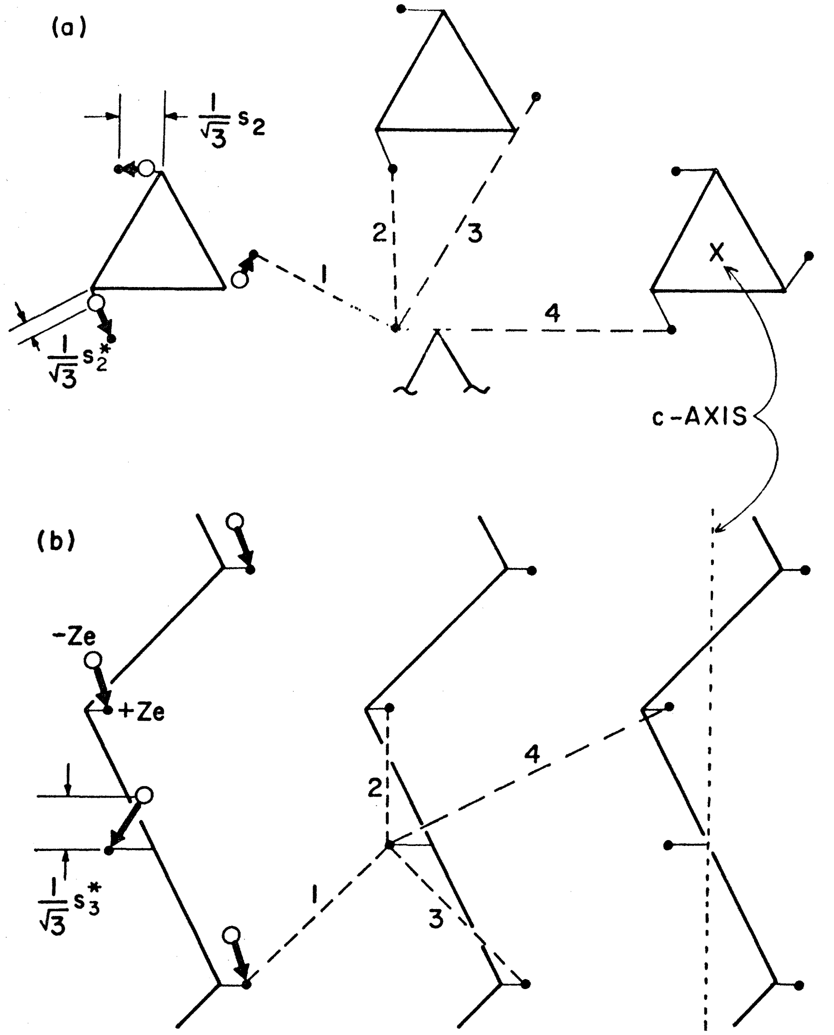

FIG. 2. A_2-symmetry optical mode: (a) top view (viewed along the c axis); (b) side view (viewed $\perp c$). Solid dots represent displaced cores; open circles, displaced shells. The numbered dashed lines indicate next-nearest-neighbor "interchain" bonds.

Since $e^*(A_2)\sim e$ and $Z\sim 1$, we see from (4.12) that $a_{32}\sim 1$, so that $s_3^*\sim s_2$. Thus a chain-twisting atomic displacement (s_2) induces an axial shell displacement (s_3^*) of comparable magnitude. The mechanical energy of the vibration resides, of course, with the massive cores, i.e., with s_2. We may regard that the electromagnetic character of the mode resides with s_3^* which is responsible for the first-order moment, the macroscopic electric polarization of the lattice.

The coefficient a_{32} is a measure of the deformability, under chain rotation, of the charge distribution. When a_{32} vanishes, then so does $e^*(A_2)$ and, from (4.3), a_{22} is unity; shells and cores then move together and we have, in effect, neutral rigid atoms. This occurs when $D_{22}^{cs}=-D_{22}^{ss}$. If, in addition, $D_{22}^{cc}=D_{22}^{ss}$, then a relation of the form of (3.3) obtains for $ij=22$, indicating invariance of the dynamical matrix under a rigid chain rotation ($\mathbf{e}_2+\mathbf{e}_2^*$). In this case, which corresponds to the limit of negligible interactions between chains, λ_{22} also vanishes.

The axial shell displacement s_3^* shown in Fig. 2 corresponds to a particular choice of sign (positive in our coordinate convention) for a_{32}, which can deviate from zero (the rigid-atom value) in either direction. This sign is not determined by ir measurements. If we consider the electronic charge to be concentrated along the bond directions, and assume that overlap repulsion causes a charge transfer from bonds under compression to bonds under tension, then the contributions to a_{32} of transfer within the NNN bond pairs 1–4 and 2–3 are, respectively, positive and negative. Molecular-orbital arguments[22] indicate that in the vicinity of each atom more charge is located along bonds 1 and 4 than bonds 2 and 3, hence the (positive) choice of sign shown in Fig. 2.

This question of the sign of a_{32}, and hence of $e^*(A_2)$, is closely analogous to the question of the sign of the deviation of e^*/e from unity for the alkali halides.[10]

---

[22] S. Tutihasi and I. Chen, Phys. Rev. 158, 623 (1967).

There $e^*/e<1$ because the dynamic-charge contribution to e^* is dominated by the part arising from the deformability of the negative ion. The concentration of charge about the negative ion in that case is directly analogous to the concentration of charge along particular bond directions in the present case. In both cases the dynamic charge is a net result of contributions of opposite sign arising from different portions of the charge distribution. Of course, for the alkali halides the dynamic charge merely provides a correction to the rigid-ion value of e^*, while for the elemental crystals discussed here it is the whole story.

5. E-SYMMETRY OPTICAL MODES

For the E modes it suffices to consider one of the identical 6×6 blocks on the diagonal of $\mathbf{D}$, provided that we keep in mind that for each solution

$$\mathbf{u}=s_4\mathbf{e}_4+s_5\mathbf{e}_5+s_6\mathbf{e}_6+s_4{}^*\mathbf{e}_4{}^*+s_5{}^*\mathbf{e}_5{}^*+s_6{}^*\mathbf{e}_6{}^* \quad (5.1)$$

there is a degenerate solution obtained by replacing $\mathbf{e}_i$ by $\mathbf{e}_{i+3}$ and $\mathbf{e}_j{}^*$ by $\mathbf{e}_{j+3}{}^*$.

The relations between shell and core displacements, obtained by setting $m^*=0$ as before, are

$$\begin{aligned} s_4{}^*&=s_4+a_{45}s_5+a_{46}s_6\,,\\ s_5{}^*&=\qquad a_{55}s_5+a_{56}s_6\,,\\ s_6{}^*&=\qquad a_{65}s_5+a_{66}s_6\,. \end{aligned} \quad (5.2)$$

Three of the nine coupling coefficients are found to be independent of $\mathbf{D}$;

$$a_{44}=1\,,\quad a_{54}=a_{64}=0\,. \quad (5.3)$$

The expressions for the two coefficients which will appear in the effective charge tensor are

$$a_{45}=\frac{1}{\Delta}\begin{vmatrix} D_{45}{}^{cc} & D_{45}{}^{cc} & D_{46}{}^{cc}\\ -D_{55}{}^{cs} & D_{55}{}^{ss} & D_{56}{}^{ss}\\ -D_{56}{}^{cs} & D_{56}{}^{ss} & D_{66}{}^{ss} \end{vmatrix}\,,$$

$$a_{46}=\frac{1}{\Delta}\begin{vmatrix} D_{46}{}^{cc} & D_{45}{}^{cc} & D_{46}{}^{cc}\\ -D_{56}{}^{cs} & D_{55}{}^{ss} & D_{56}{}^{ss}\\ -D_{66}{}^{cs} & D_{56}{}^{ss} & D_{66}{}^{ss} \end{vmatrix}\,,$$

where

$$\Delta=\begin{vmatrix} D_{44}{}^{cc} & D_{45}{}^{cc} & D_{46}{}^{cc}\\ D_{45}{}^{cc} & D_{55}{}^{ss} & D_{56}{}^{ss}\\ D_{46}{}^{cc} & D_{56}{}^{ss} & D_{66}{}^{ss} \end{vmatrix}\,. \quad (5.4)$$

One of three solutions corresponds to an acoustical mode:

$$\omega=0\,,\quad s_5=s_5{}^*=s_6=s_6{}^*=0\,,\quad s_4=s_4{}^*\,. \quad (5.5)$$

For the remaining two solutions, representing optical modes, $s_4=0$, while the other five E-symmetry coordinates are all, in general, nonvanishing. From (3.7) and the definitions of Table I, the electric moment associated with the $\mathbf{u}$ of (5.1) is $\mathbf{p}=p_x\hat{x}$, with

$$p_x=\sqrt{3}Ze(s_4-s_4{}^*)\,. \quad (5.6)$$

Thus $\mathbf{p}$ vanishes for the acoustical mode, and for the optical modes

$$\begin{aligned} p_x&=-\sqrt{3}Zes_4{}^*\\ &=-\sqrt{3}Ze(a_{45}s_5+a_{46}s_6)\,. \end{aligned} \quad (5.7)$$

The actual optical-mode eigenvectors, which we denote as $\mathbf{e}_\alpha$ and $\mathbf{e}_\beta$, will, in general, mix core displacements $\mathbf{e}_5(\perp c)$ and $\mathbf{e}_6(\|c)$. Introducing a mixing parameter α we can write, by orthonormality,

$$\begin{aligned} \mathbf{e}_\alpha&=\alpha\mathbf{e}_5+(1-\alpha^2)^{1/2}\mathbf{e}_6\,,\\ \mathbf{e}_\beta&=(1-\alpha^2)^{1/2}\mathbf{e}_5-\alpha\mathbf{e}_6\,. \end{aligned} \quad (5.8)$$

By expressing the moment $\mathbf{p}$ induced by core displacement $s_\alpha\mathbf{e}_\alpha$ as $e^*(E_\alpha)s_\alpha\hat{x}$, and similarly for $s_\beta\mathbf{e}_\beta$, we obtain the effective charges for the optical modes of E symmetry:

$$\begin{aligned} e^*(E_\alpha)&=-\sqrt{3}Ze[\alpha a_{45}+(1-\alpha^2)^{1/2}a_{46}]\\ e^*(E_\beta)&=-\sqrt{3}Ze[(1-\alpha^2)^{1/2}a_{45}-\alpha a_{46}]\,. \end{aligned} \quad (5.9)$$

[While α, and for that matter $\omega(E_\alpha)$ and $\omega(E_\beta)$, can be calculated in terms of the 12 D_{ij}'s appearing in the 6×6 E block, the resulting complex expressions are unilluminating and will be omitted here.]

It is interesting to consider the form of expressions (5.9) in the light of the following experimental observations: For both Se and Te, the effective charge of one E vibration is very small, an order of magnitude less than that of the other (for which $|e^*|\sim e$).[2,4] In (5.9) the effective charges appear as the sum of two terms which, independent of the relative signs of α, a_{45}, and a_{46}, interfere constructively in one case and destructively in the other. Thus one set of circumstances concordant with experiment consists of comparable coupling coefficients ($|a_{45}|\approx|a_{46}|$) and comparable components $\|$ and $\perp$ to c [$|\alpha|\approx|(1-\alpha^2)^{1/2}|\approx1/\sqrt{2}$]. More generally, if we write

$$\begin{aligned} e^*(E_\alpha)&=e_0{}^*\cdot(1+\gamma\eta)\,,\\ e^*(E_\beta)&=e_0{}^*\cdot(\gamma-\eta)\,, \end{aligned} \quad (5.10)$$

where $e_0{}^*\equiv-\sqrt{3}Ze\alpha a_{45}$, $\gamma\equiv(1-\alpha^2)^{1/2}/\alpha$, $\eta\equiv a_{46}/a_{45}$, then the experimental results require that $\gamma\approx\eta$ or $-\eta^{-1}$. The set of circumstances described just above corresponds to $|\gamma|\approx|\eta|\approx1$.

For (5.4) we see that in terms of dynamical matrix elements η simplifies to $D_{46}{}^{cc}/D_{45}{}^{cc}$ when $D_{55}{}^{cs}/D_{55}{}^{ss}=D_{56}{}^{cs}/D_{56}{}^{ss}=D_{66}{}^{cs}/D_{66}{}^{ss}=\zeta$. Setting $\zeta=1$ is equivalent to an assumption that the core-shell interactions occur via the shells.[23] For $\zeta=-1$, $a_{45}=a_{46}=0$ and both

---

[23] R. A. Cowley, W. Cochran, B. N. Brockhouse, and A. D. B. Woods, Phys. Rev. **131**, 1030 (1963).

E-mode effective charges vanish. In fact, in this case the only nonvanishing coupling coefficients are $a_{44}=a_{55}=a_{66}=1$, which describes neutral rigid atoms. If $\zeta=-1$ and, in addition, the same relations hold with $D_{ij}{}^{ss}$ replaced by $D_{ij}{}^{cc}$, the E-symmetry eigenfrequencies vanish as well as the effective charges.

6. EFFECTIVE CHARGE TENSOR, POLARIZABILITY, AND RAMAN SCATTERING

The results of the preceding sections enable us to construct the effective charge tensor $\mathbf{B}=\partial\mathbf{p}/\partial\mathbf{u}$ which connects the atomic displacements $\mathbf{u}=s_1\mathbf{e}_1+s_2\mathbf{e}_2+\cdots+s_9\mathbf{e}_9$ with the first-order electric moment $\mathbf{p}=p_x\hat{x}+p_y\hat{y}+p_z\hat{z}$. In the symmetrized coordinates of Table I, this tensor (showing only nonvanishing matrix elements) has been found to be

$$\mathbf{B}=-\sqrt{3}Ze\cdot\begin{bmatrix} \cdot & \cdot & \cdot & \cdot & a_{45} & a_{46} & \cdot & \cdot & \cdot \\ \cdot & \cdot & \cdot & \cdot & \cdot & \cdot & \cdot & a_{45} & a_{46} \\ \cdot & a_{32} & \cdot & \cdot & \cdot & \cdot & \cdot & \cdot & \cdot \end{bmatrix}. \qquad (6.1)$$

$\mathbf{B}$ contains five nonvanishing elements, three of them independent, corresponding to the five ir-active eigenvibrations and the three ir-active eigenfrequencies.[24]

The three coupling coefficients appearing in (6.1), defined in (4.3) and (5.2), are those which specify the acoustical (translational) shell displacements (s_3^*,s_4^*,s_7^*) induced by the A_2+2E optical core displacements (s_2,s_5,s_6,s_8,s_9). In (4.3) and (5.4) we have expressed these coefficients in terms of shell-model dynamical matrix elements.

Besides the polarization $\mathbf{Bu}$ induced by lattice displacements, the present approximation allows us to discuss the ordinary polarizability describing the response $\mathbf{A}\boldsymbol{\varepsilon}$ to an electric field $\boldsymbol{\varepsilon}$. For trigonal symmetry the polarizability tensor possesses two independent elements, $A_{xx}=A_{yy}$ and A_{zz}.[25] Working in the A_2-symmetry manifold, we will derive shell-model expressions for $A_{zz}(\omega=0)$ and $A_{zz}(\omega=\infty)$, the static and optical polarizabilities for $\boldsymbol{\varepsilon}\parallel c$.

The response to a stationary field $\epsilon_z\hat{z}$ can be found by setting the LHS of (4.1) equal to zero ($\omega=0$) and adding to the RHS the term

$$\begin{bmatrix} 0 \\ -\sqrt{3}Ze\epsilon_z \\ 0 \\ +\sqrt{3}Ze\epsilon_z \end{bmatrix}.$$

Solving for the unit-cell moment p_z by means of (4.10), and recognizing that $A_{zz}=p_z/v\epsilon_z$, where v is the unit-cell volume, we obtain for the static polarizability

$$A_{zz}(0)=\frac{3(Ze)^2[D_{22}{}^{cs^2}-D_{22}{}^{cc}D_{22}{}^{ss}]}{m\omega^2(A_2)v[D_{23}{}^{cc^2}-D_{22}{}^{ss}D_{33}{}^{cc}]}. \qquad (6.2)$$

Equations (4.5–6) have been used to slightly simplify the form of (6.2).

For the high-frequency polarizability in the crystal's transparent regime, we consider a frequency assumed to be much greater than phonon frequencies but much smaller than electronic frequencies, $\omega^2(A_2)\sim D_{ij}/m\ll\omega^2\ll D_{ij}/m^*$. At this frequency the cores do not respond and may be regarded as fixed; for convenience we choose $s_2=s_3=0$, although as we shall see the choice does not matter. We are then left with a 2×2 secular equation in s_2^* and s_3^*, and readily obtain the optical polarizability

$$A_{zz}(\infty)=\frac{3(Ze)^2D_{22}{}^{ss}}{v[D_{22}{}^{ss}D_{33}{}^{cc}-D_{23}{}^{cc^2}]}. \qquad (6.3)$$

The increase in A_{zz} between optical and low frequencies is due to the absorption associated with the intervening A_2-mode reststrahlen band. With the aid of (4.5–6) for $\omega(A_2)$ and (4.3;4.12) for $e^*(A_2)$, we can verify that the polarizabilities of (6.2–3) satisfy, as they must, the relation[26]

$$A_{zz}(0)-A_{zz}(\infty)=e^{*2}(A_2)/m\omega^2(A_2)v. \qquad (6.4)$$

In the presence of both atomic displacements $\mathbf{u}$ and electric field $\boldsymbol{\varepsilon}$, the polarization contains a second-order term $\mathbf{C}\mathbf{u}\boldsymbol{\varepsilon}$ in addition to the terms $\mathbf{A}\boldsymbol{\varepsilon}+\mathbf{B}\mathbf{u}$ discussed above. This bilinear term is responsible for Raman scattering: $\mathbf{Cu}$ is equivalent to a polarizability change induced by the atomic displacements. We have been able to discuss the second-rank tensors $\mathbf{A}$ and $\mathbf{B}$ with the model treated in this paper, but cannot do so for the third-rank tensor $\mathbf{C}$. Thus in the derivation of (6.3) we find the result to be independent of s_2 and s_3; the optical polarizability is not modulated by the lattice vibrations and there is no Raman scattering.[27] The reason for this is simple. The shell-model equations of motion in the harmonic approximation are linear in $\mathbf{u}$ as well as in $\boldsymbol{\varepsilon}$. Solutions superimpose so that the response to a field $\boldsymbol{\varepsilon}$, and therefore the polarizability, is unaffected by the presence or absence of displacements $\mathbf{u}$. In order to obtain Raman scattering (nonvanishing $\mathbf{C}$) we would need to extend the approximation to include such quantities as displacement-dependent shell-shell springs, $D_{ij}{}^{ss}\rightarrow D_{ij}{}^{ss}+D_{ijk}{}^{ssc}s_k$.

7. LONG-RANGE ELECTROSTATIC FORCES

The oscillating dipoles set up at the atomic sites by the lattice vibrations, such as those shown for the A_2 optical mode in Fig. 2, contribute a long-range electrostatic interaction to the dynamical matrix.[7] In the shell

---

[24] Reference 6, Sec. 3.

[25] J. F. Nye, *Physical Properties of Crystals* (Oxford University Press, London, 1957), Appendix E.

[26] Reference 7, Sec. 7; E. Burstein, in *Proceedings of the International Conference on Lattice Dynamics, Copenhagen, 1963*, edited by R. F. Wallis (Pergamon Press, Ltd., London, 1965), p. 315.

[27] The case worked out in (6.3) is actually a bad choice for demonstrating this point since the A_2 mode is Raman-inactive by symmetry. However, the same negative result (no Raman scattering) is obtained by working out the corresponding shell-model equations for the Raman-active A_1 and E modes.

model this dipolar interaction is prescribed by the charge assignment Z and by the detailed geometry of the crystal structure. In this section we calculate the long-range Coulomb interaction matrix at $q=0$ for both Se and Te. Long-range forces, omitted from previous force-constant treatments,[4,9] are important in determining the zone-center optical phonons in these two crystals. This is in marked contrast to the germanium-family elemental crystals. Not only is there no vibration-induced macroscopic polarization in Ge,[5,6] but at $q=0$ there is also no microscopic electrostatic interaction because each atomic dipole sees a tetrahedrally-symmetric dipole array which exerts no force upon it.[28] For Se and Te, the dipole-dipole interaction at the zone center is not suppressed by symmetry.

The field exerted on a dipole by all the other dipoles in the crystal is referred to as the exciting field (XF),[29] and we will denote the corresponding contribution to the dynamical matrix by $\mathbf{D}^{XF}$. The lattice sum for $\mathbf{D}^{XF}(\mathbf{q})$, expressed in a form which exploits Ewald's θ-function transformation, has been derived by Born and Huang.[29] BH present the result in condensed form. Explicitly written out in full for purposes of calculation, it is as follows:

$$D_{k\alpha,k'\alpha'}{}^{XF}(\mathbf{q})=-Z_kZ_{k'}e^2Q_{k\alpha,k'\alpha'}(\mathbf{q})\,; \tag{7.1}$$

$$\begin{aligned}Q_{k\alpha,k'\alpha'}(\mathbf{q})=&-4\pi v^{-1}q_\alpha q_{\alpha'}q^{-2}\exp(-\pi^2q^2\rho^{-2})+\delta_{kk'}\delta_{\alpha\alpha'}\tfrac{4}{3}\pi^{-1/2}\rho^3+{\textstyle\sum_l}'\,\{3x_\alpha x_{\alpha'}x^{-5}\operatorname{erfc}(\rho x)-\delta_{\alpha\alpha'}x^{-3}\operatorname{erfc}(\rho x)\\&+6\pi^{-1/2}\rho x_\alpha x_{\alpha'}x^{-4}\exp(-\rho^2x^2)+4\pi^{-1/2}\rho^3x_\alpha x_{\alpha'}x^{-2}\exp(-\rho^2x^2)-\delta_{\alpha\alpha'}2\pi^{-1/2}\rho x^{-2}\exp(-\rho^2x^2)\}\exp(-2\pi i\mathbf{q}\cdot\mathbf{x})\\&-4\pi v^{-1}{\textstyle\sum_{\mathbf{h}}}'\,(h_\alpha+q_\alpha)(h_{\alpha'}+q_{\alpha'})|\mathbf{h}+\mathbf{q}|^{-2}\exp[-\pi^2\rho^{-2}|\mathbf{h}+\mathbf{q}|^2+2\pi i\mathbf{h}\cdot\mathbf{x}(0,kk')].\end{aligned} \tag{7.2}$$

The matrix $\mathbf{Q}$, with the dimensions of reciprocal volume, contains the dependence on the atomic positions and is the same as BH's $\mathbf{Q}$ save for the first term, which they split off to discuss separately. At $q=0$ this term corresponds to the macroscopic field and will not be considered here as it vanishes for transverse vibrations. In (7.2) $\mathbf{x}$ denotes $\mathbf{x}(l,kk')\equiv\mathbf{x}(l,k)-\mathbf{x}(0,k')$, $\mathbf{h}$ denotes a reciprocal lattice vector, and ρ is the θ function dividing point, an arbitrary parameter (with dimensions of reciprocal length) chosen to obtain rapid convergence of the two sums. The primes indicate that in the lattice sum the term $l=l'$ is omitted when $k=k'$ and in the reciprocal lattice sum the term $h=0$ is omitted.

There are three structure parameters needed to fix the atomic positions in Se and Te: the unit cell dimensions a and c, and the bond length b. These are indicated in Fig. 1 and their room temperature values are given in Table II.[30] It is convenient to work with the quantities d_1, d_2, and d_3 given by $\frac{1}{2}a$, $\frac{1}{2}[b^2-(\frac{1}{3}c)^2]^{1/2}$, and $\frac{1}{3}c$, respectively.

With Table II as input data for the sums of (7.2), $\mathbf{Q}$ has been numerically calculated with the aid of an IBM 7044 computer. The program was written to obtain $\mathbf{Q}(\mathbf{q})$, but here we discuss only $\mathbf{Q}(0)$; results for the full zone will be presented later. The program was tested by checking that it yields $Q_{k\alpha,k'\alpha'}=(4\pi/3v)\delta_{\alpha\alpha'}$ for a cubic crystal. For both Se and Te it was found that sums over ≈ 500 lattice vectors, using $\rho\approx 0.4(\text{Å})^{-1}$, yielded good convergence. Convergence was also checked by comparing components connected by symmetry.

In symmetrized coordinates the $\mathbf{Q}$ matrices have the form shown in Table I. The ten independent elements of $\mathbf{Q}(0)$ for Se and Te, calculated as described above, are presented in Table III. The shell-model $\mathbf{D}^{XF}(0)$ is then specified by (7.1):

$$\mathbf{D}^{XF}=-(Ze)^2\begin{pmatrix}\mathbf{Q} & -\mathbf{Q}\\ -\mathbf{Q} & \mathbf{Q}\end{pmatrix}. \tag{7.3}$$

The Coulomb coefficients for Se, because of the smaller spacings in this crystal, are somewhat larger than for Te. However the appropriate value of Z in (7.3) is certainly larger for Te than for Se by virtue of the former's greater atomic number and electronic

TABLE II. Structure parameters.[a]

Crystal	Unit-cell dimensions (Å) a	c	Bond length (Å) b	Definitions of d_i
Se	4.366	4.954	2.373	$d_1=\frac{1}{2}a$; $d_3=\frac{1}{3}c$;
Te	4.457	5.929	2.835	$d_2=\frac{1}{2}[b^2-(\frac{1}{3}c)^2]^{1/2}$

[a] See Ref. 30.

TABLE III. Electrostatic interaction matrix elements in 10^{-25} cm^{-3}.

Matrix element	Se	Te
Q_{11}	−0.675	−0.060
Q_{22}	1.387	0.813
Q_{23}	0.688	0.268
Q_{33}	2.117	1.476
Q_{44}	1.246	1.110
Q_{45}	−0.486	−0.189
Q_{46}	0.516	0.218
Q_{55}	−0.712	−0.753
Q_{56}	−0.972	−0.378
Q_{66}	0.356	0.376

---

[28] Reference 7, Sec. 9; W. Cochran, Proc. Roy. Soc. (London) **A253**, 260 (1959).

[29] Reference 7, Sec. 30; P. P. Ewald, Ann. Physik **54**, 519 (1917); **54**, 557 (1917); **64**, 253 (1921).

[30] P. Cherin and P. Unger, Inorg. Chem. **6**, 1589 (1967); Acta Cryst. **23**, 670 (1967).

TABLE IV. Central-force shell-model dynamical matrix elements.

Symmetry	Matrix element	K	Coefficients of the short-range parameters			
			$R_{\mathrm{NN}}{}^{cc}$	$R_{\mathrm{NN}}{}^{cs}$	$R_{\mathrm{NNN}}{}^{cc}$	$R_{\mathrm{NNN}}{}^{cs}$
A_1	$D_{11}{}^{cc}$	-1	$12d_2{}^2$	$6d_2{}^2$	$6(\sqrt{3}d_1-2d_2)^2$	$10d_1{}^2+12d_2{}^2-12\sqrt{3}d_1d_2$
	$D_{11}{}^{cs}$	$+1$		$6d_2{}^2$		$8d_1{}^2+12d_2{}^2-12\sqrt{3}d_1d_2$
A_2	$D_{22}{}^{cc}$	-1		$2d_2{}^2$	$6d_1{}^2$	$6d_1{}^2+4d_2{}^2-4\sqrt{3}d_1d_2$
	$D_{22}{}^{cs}$	$+1$		$-2d_2{}^2$		$4d_2(\sqrt{3}d_1-d_2)$
	$D_{23}{}^{cc}$			$2d_2d_3$		$-2d_3(\sqrt{3}d_1-2d_2)$
	$D_{33}{}^{cc}$	-1		$2d_3{}^2$		$4d_3{}^2$
E	$D_{44}{}^{cc}$	-1		$4d_2{}^2$		$8(d_1{}^2+d_2{}^2-\sqrt{3}d_1d_2)$
	$D_{45}{}^{cc}$			$-\sqrt{2}d_2d_3$		$\sqrt{2}d_3(\sqrt{3}d_1-2d_2)$
	$D_{46}{}^{cc}$			$2d_2{}^2$		$2d_1{}^2+4d_2{}^2-4\sqrt{3}d_1d_2$
	$D_{55}{}^{cc}$	-1	$3d_3{}^2$	$2d_3{}^2$	$6d_3{}^2$	$4d_3{}^2$
	$D_{55}{}^{cs}$	$+1$		$d_3{}^2$		$2d_3{}^2$
	$D_{56}{}^{cc}$		$3\sqrt{2}d_2d_3$	$\sqrt{2}d_2d_3$	$-3\sqrt{2}d_3(\sqrt{3}d_1-2d_2)$	$-\sqrt{2}d_3(\sqrt{3}d_1-2d_2)$
	$D_{56}{}^{cs}$			$2\sqrt{2}d_2d_3$		$-2\sqrt{2}d_3(\sqrt{3}d_1-2d_2)$
	$D_{66}{}^{cc}$	-1	$6d_2{}^2$	$4d_2{}^2$	$12(d_1{}^2+d_2{}^2-\sqrt{3}d_1d_2)$	$8(d_1{}^2+d_2{}^2-\sqrt{3}d_1d_2)$
	$D_{66}{}^{cs}$	$+1$		$2d_2{}^2$		$4(d_1{}^2+d_2{}^2-\sqrt{3}d_1d_2)$

polarizability. For Te the effective charges of the ir-active modes, proportional to Z, are approximately twice those for Se.[2,4] Since $D_{ij}{}^{XF}$ is proportional to Z^2 as well as to Q_{ij}, the exciting field is larger in Te. From Table III and (7.3), the elements of $\mathbf{D}^{XF}$ relevant to the A_2 optical mode are $\approx(1\text{–}4)\times10^4$ g sec^{-2} for $Z\approx1$. Since $m\omega^2(A_2)\approx(5\text{–}6)\times10^4$ g sec^{-2} for the two crystals, it is clear that long-range forces significantly affect this vibration.

8. SHORT-RANGE CENTRAL FORCES

To illustrate some of the results of Secs. 4 and 5 obtained with a general, symmetrized, shell-model dynamical matrix, we now consider a very simple model which assumes, for the short-range interactions, central forces between nearest and next-nearest shell-model neighbors. Interaction between core and shell at the same site is taken to be isotropic with force constant K. The potentials describing interactions between sites are assumed to be of the following form, illustrated for the interaction between a core on one site and a shell at a next-nearest neighbor (NNN) site:

$$\Psi_{\mathrm{NNN}}{}^{cs}=\Psi_{\mathrm{NNN}}{}^{cs}(|\mathbf{x}(ll',kk')+\mathbf{u}^c(l,k)-\mathbf{u}^s(l',k')|^2). \quad (8.1)$$

These interactions will be specified by the six quantities $R_{\mathrm{NN}}{}^{cc}$, $R_{\mathrm{NN}}{}^{cs}$, $R_{\mathrm{NN}}{}^{ss}$, $R_{\mathrm{NNN}}{}^{cc}$, $R_{\mathrm{NNN}}{}^{cs}$, and $R_{\mathrm{NNN}}{}^{ss}$, where, for the example of (8.1),

$$R_{\mathrm{NNN}}{}^{cs}=4\Psi_{\mathrm{NNN}}{}^{cs\prime\prime}(|\mathbf{x}(ll',kk')|^2). \quad (8.2)$$

In terms of these central-force parameters and the geometric factors of Table II, the short-range contribution to the symmetrized dynamical matrix is as shown in Table IV. This table presents the short-range contribution to 15 of the 20 shell-model matrix elements in terms of 5 of the 7 force constants; the remaining matrix elements ($D_{ij}{}^{ss}$ for $ij=11, 22, 55, 56, 66$) and force constants ($R_{\mathrm{NN}}{}^{ss}$ and $R_{\mathrm{NNN}}{}^{ss}$) are obtained by interchanging c and s in the expressions for $D_{ij}{}^{cc}$. The total matrix elements are obtained by adding short-range and long-range contributions, e.g.,

$$D_{33}{}^{cc}=-K+2d_3{}^2R_{\mathrm{NN}}{}^{cs}+4d_3{}^2R_{\mathrm{NNN}}{}^{cs}-Z^2e^2Q_{33}.$$

In Sec. 4 we showed that $e^*(A_2)$ is proportional to the coupling coefficient a_{32}, and that a_{32} vanishes when $D_{22}{}^{cs}+D_{22}{}^{ss}$ vanishes. In terms of the central-force model $D_{22}{}^{cs}+D_{22}{}^{ss}$ becomes $6d_1{}^2(R_{\mathrm{NNN}}{}^{cs}+R_{\mathrm{NNN}}{}^{ss})$ demonstrating, as mentioned earlier, that the A_2-mode dynamic charge requires the presence of next-nearest neighbor interactions; $e^*(A_2)=0$ if $R_{\mathrm{NNN}}{}^{cs}=R_{\mathrm{NNN}}{}^{ss}=0$. In Sec. 5 we found that the relevant coupling coefficients for the E modes vanish if $D_{ij}{}^{cs}+D_{ij}{}^{ss}=0$ for $ij=55, 56, 66$. For this to occur in the present context, both nearest and next-nearest-neighbor interactions would have to vanish, as can be seen by examining Table IV.

Returning to the A_2 mode, it is easy to show that $\omega(A_2)$ vanishes if the three R_{NNN}'s vanish; we have already seen that $e^*(A_2)$ vanishes if two of the R_{NNN}'s vanish. This points out the intimate connection between dynamic charge and the bonding interactions responsible for restoring forces.

With Table IV and the results of the previous section one could construct a shell-model dynamical matrix containing eight parameters: $Z, K, R_{\mathrm{NN}}{}^{cc}, \cdots, R_{\mathrm{NNN}}{}^{ss}$. Optical experiments alone can provide nine quantities: four optical-mode frequencies $[\omega(A_1)$, $\omega(A_2)$, $\omega(E)$, $\omega(E)]$, three effective charges $[e^*(A_2)$, $e^*(E)$, $e^*(E)]$, and two optical polarizabilities $[A_{xx}(\infty)$, $A_{zz}(\infty)]$. Expressions for these quantities in terms of shell-model matrix elements have been discussed in Secs. 4–6 of this paper. There are also six elastic constants for D_3-symmetry crystals, and some of these have been measured for Te and Se. The elastic constants can similarly be expressed in terms of matrix elements. Geick and Schröder,[4] using Hulin's model for the short-range forces,[9] have performed a rigid-atom force-constant fit to the optical frequencies and certain elastic constants for the two crystals. (Effective charges and polarizabilities are, of course, outside the scope of a rigid-atom model for an elemental crystal.) The work of these authors indicates that an adequate model for the short-range interactions must go beyond nearest- and next-nearest central-force interactions. We are presently refining our treatment of short-range forces so that, by means of these and the results for the long-range interaction, we can calculate the optical properties mentioned above and, in addition, extend the shell-model analysis over the full Brillouin zone.

9. SUMMARY

Trigonal Se and Te, with $s=3$, belong to the simplest class of reststrahlen-displaying elemental crystals. We have performed a shell-model analysis of their $q=0$ optical phonons, using the most general dynamical matrix consistent with crystal symmetry and translational invariance. The dynamic charges associated with the ir-active modes have been derived in terms of shell-model matrix elements, and the effective charge tensor constructed in symmetrized coordinates.

The effective charge tensor for Se and Te contains three independent entries which correspond to three of the coupling coefficients appearing in the theory. These dimensionless quantities specify the shell displacements induced by displacements of the cores. In the shell model for an elemental crystal the vibration-induced macroscopic polarization is due entirely to the shell motion. The important coupling coefficients are those connecting acoustical shell displacements with optical core displacements; in the present context they are a_{32} for A_2 symmetry, a_{45} and a_{46} for E symmetry.

For the A_2 optical vibration, the chain-rotational core motion induces an axial shell motion responsible for the first-order moment, thereby accounting for the interaction with light polarized parallel to c of a mode in which all of the atomic displacements are perpendicular to the c axis. The dynamic charge of this mode, $e^*(A_2)=-\sqrt{3}Zea_{32}$, depends upon the presence of NNN interactions between chains, as does the eigenfrequency $\omega(A_2)$; both $e^*(A_2)$ and $\omega(A_2)$ vanish in the limit of isolated chains. In a bond picture, a_{32} may be understood in terms of charge transfer between NNN bonds. We assign a sign to a_{32}, and therefore to $e^*(A_2)$, by a molecular orbital argument.

The analysis for the E modes, which occur in degenerate pairs and mix motions parallel and perpendicular to c, yields more complex results. The relevant coupling coefficients, a_{45} and a_{46}, are combined in the two $e^*(E)$'s in a manner which leads to reenforcement in one case, cancellation in the other. The latter provides a means for understanding the very small oscillator strength observed for one of the two E-mode pairs in measurements on both Se and Te.

Dielectric polarizabilities, as well as effective charges, can be treated in the present model, and we have obtained expressions for $A_{zz}(0)$ and $A_{zz}(\infty)$. Raman scattering, however, is excluded from this treatment since the harmonic-approximation shell-model equations of motion are separately linear in electric field and atomic displacement.

Unlike Ge, for Se and Te the dipole-dipole interaction at $q=0$ does not vanish. The lattice sums which enter into this long-range electrostatic interaction have been evaluated for the specific geometry of both crystals. A simple central-force model for the short-range interactions has been considered in order to illustrate some of the points discussed.

ACKNOWLEDGMENTS

The authors are indebted to Dr. H. Scher and Professor E. W. Montroll for valuable discussions about this work, and to Dr. S. H. Chen for a copy of his important paper (Ref. 12) prior to publication.